Uranium M x-ray emission spectrum*

O. Keski-Rahkonen† and M. O. Krause
Transuranium Research Laboratory, Oak Ridge National Laboratory, Oak Ridge, Tennessee 37830
(Received 25 May 1976)

The uranium M x-ray spectrum from a thick metallic target excited by 12-keV electrons was measured by the PAX (photoelectron spectrometry for the analysis of x rays) technique. Energies of the strongest lines were obtained with an accuracy of 0.1 eV using Ag $L\beta_1$ and Ag $L\alpha_1$ as standards. Widths of the uranium lines were obtained by deconvoluting the measured Voigt profiles, and the experimental values were found to agree satisfactorily with McGuire's Hartree-Slater predictions. Natural widths of 4.0(3) and 3.8(3) eV were derived for the M_4 and M_5 levels, respectively, and the energies of the M_4, M_5, N_2, and N_3 levels in uranium metal were determined. Relative intensities of the M lines were measured, and branching ratios were found to be in fair agreement with relativistic Hartree-Slater predictions. The satellite structures of the $M\alpha_1$ and $M\beta$ lines were interpreted in terms of the pertinent multiple-hole configurations. Finally, an approximate analytic expression for the Voigt half-width and its graphical representation are given.

I. INTRODUCTION

Although the M x-ray emission spectrum of uranium has been recorded repeatedly,[1,2] widths and intensities of the lines have not been previously determined, and the accuracy of the x-ray energy values averaged[3] from the various measurements has remained low. Using the PAX method[4,5] (photoelectron spectrometry for the analysis of x rays), we remeasured the uranium M spectrum to determine linewidths and relative intensities, for which calculations have recently become available,[6-10] and to improve the accuracy of the energy values. A brief, preliminary report of this work has been given previously.[11]

II. EXPERIMENTAL

Since the principle and characteristics of the PAX method have been described elsewhere,[4,5] only essential features and instrumental details pertaining to this work will be given here. In particular, we describe the procedure and setup employed for an accurate energy determination and present a simple approximation of the Voigt integral half-width, which allows a convenient determination of the natural linewidth from the measured peak contour.

A. General

X rays are converted into photoelectrons from a gaseous source, such as neon, in the arrangement shown schematically in Fig. 1. The electrons that pass through the acceleration slits are dispersed in an electrostatic, spherical sector-plate energy analyzer and counted individually. A spectral range is scanned at the rate of 20/sec by applying a repetitive sawtooth to each of the dc-biased sector plates and storing the signals in the memory of a multiscaler operated in synchronization with the sawtooth. The expression

$$E_{\text{kin}} = fV + gC + (\text{relativistic terms}) \quad (1)$$

relates the energy E_{kin} of the electron, upon entering the analyzer, to the bias voltage V and the channel number C of the scaler, where f is the analyzer and g the scale constant (in eV/channel).

B. Acceleration slit structure

The structure shown in Fig. 2 permits the acceleration of electrons from a gaseous source. Photons from the anode (3) enter the converter cell (10) through an 8-μm Be window (2) and a 0.6-μm Al foil (1). Electrons are born in a field-free region (10) at the potential U applied to cell walls, slits (5–7), backing plate (4), and windows (1), and are accelerated between (7) and (8) to ground potential. Up to 800 V can be applied between (7) and (8). Slits (5–9) define the azimuthal

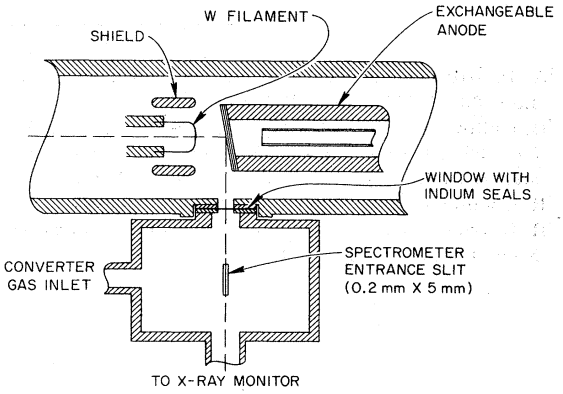

Photon Source and Converter Arrangement.

FIG. 1. Schematic of x-ray tube and photoelectron source.

apex angle to about 3° as long as eU is small compared with the initial photoelectron energy.

C. Energy measurement

The energy balance for a photoelectron ejected from an atomic level with binding energy E_B by a photon $h\nu$ and accelerated through a potential difference U is given by

$$h\nu + eU = E_{\text{kin}} + E_r + E_B + e\phi, \tag{2}$$

where E_{kin} is the kinetic energy following acceleration, ϕ the potential due to space and surface charges in the source (Fig. 2), e the electron charge, and E_r the recoil energy of the converter atom. For an electron observed perpendicular to the photon direction, E_r is approximately

$$E_r = (m/M)(h\nu - E_B), \tag{3}$$

where m and M are the electron and atomic masses, respectively.

Assuming two photons, $h\nu_1$ and $h\nu_0$, are converted by the same level, Eqs. (1) to (3) yield then for the difference $\Delta h\nu$ the relation

$$\Delta h\nu = h\nu_1 - h\nu_0 = (1 + m/M)(-e\Delta U + \Delta E_{\text{kin}})$$
$$= (1 + m/M)(-e\Delta U + f\Delta V + g\Delta C). \tag{4}$$

Thus, using a suitable x-ray standard, $h\nu_0$, the energy determination based on Eq. (4) requires only a single measurement, that of ΔU, provided the condition $|e\Delta U| \approx \Delta E_{\text{kin}}$ is met. This condition is equivalent to $\Delta V = 0$ (plate voltages constant), and $\Delta C \approx 0$ (peak positions in the same or nearby channels), and implies no need for precise values of f and g. While Eq. (4) describes the preferred mode for energy measurements of strong lines,

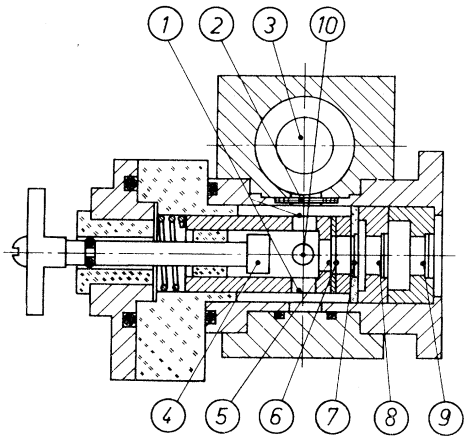

FIG. 2. View of acceleration slit structure and x-ray anode (3), showing converter gas cell (10) and slits (5)–(9). Details in text.

the relativistic form[12] of Eq. (4)

$$\Delta h\nu = (1 + m/M)[f\Delta V + g\Delta C + f^2\Delta V(V_1 + V_0)/2mc^2 + (\text{smaller terms})] \tag{5}$$

may be applied to determine the energies of weak lines using $\Delta V \neq 0$ and $\Delta U = U_1 = U_0 = 0$ [ΔU dropped from Eq. (5)]. In this work $M\alpha$ and $M\beta$ energies were obtained in the constant-plate-voltage mode [Eq. (4)], and the other M lines in the constant-acceleration mode [Eq. (5)].

D. Sources of errors in the energy measurement

The error in the measured energy $h\nu_1$ is composed of the error of the standard and the errors in the parameters of Eq. (4). In addition the possibility of *durchgriff* (field penetration) into the source, lens effect of the slits, and space-charge fluctuations need be considered. Where possible the individual contributions were measured in auxiliary experiments or evaluated from model calculations, and power supply performance. For example, durchgriff was calculated[13] to be less than 8×10^{-6} of U; lens effects and resulting shifts in the radial distance r, at which the electrons enter the analyzer, were estimated[14,15] to cause an energy shift of less than 0.1 eV for 2 keV electrons; and space-charge fluctuations were found to contribute an error of less than 20 meV. The accuracy of the absolute voltage measurements was better than $\pm2\times10^{-5}$ of ΔU; the stability of the bias voltages was about $\pm1\times10^{-5}$ of V; the uncertainty in the energy of the standards was about 30 meV; and the uncertainty in ΔC (peak positions) amounted generally to less than ±0.1 eV in the experiment and about ±20 meV in test cases exhibiting high statistical confidence. Taking into account all error sources, except the reference error, the overall error is estimated to be $(2-5)\times10^{-5}$ in $\Delta h\nu$, or at least 20 meV for small values of $\Delta h\nu$. Experimentally, the overall performance of the calibration method was checked by measuring the energy differences $E(\text{Ne } 1s) - E(\text{Ne } 2p)$ and $E(\text{Ag } L\beta_1) - E(\text{Ag } L\alpha_1)$ and comparing our values with reference data.[16,17] We found excellent mutual agreement, verifying our estimated accuracy to about 3×10^{-5} or ≈30 meV.

E. Intensity measurement

In a PAX spectrometer that uses equal entrance and exit slits for the analyzer and no pre-acceleration, the incident photon spectrum $N(h\nu)$ is related to the measured electron spectrum $N(E)$ by[5,18]

$$N(E)\,dE = GNT\eta(1-\alpha)E\sigma_{nl}(\vec{k}, h\nu)d\Omega\, N(h\nu)\,dE, \tag{6}$$

where E is the electron energy, G a geometric factor, N the number of converter atoms, $T = T(h\nu)$ the transmission of the windows between x-ray and photoelectron source, $\eta = \eta(E)$ the detector efficiency, $\alpha = \alpha(E)$ the fraction of electrons scattered out before reaching the detector, $\sigma_{nl}(\vec{k}, n\nu)$ the differential photoionization cross section of the converter level nl, and $d\Omega$ the solid angle determined by the entrance slits.

It is evident from Eq. (6) that relative x-ray intensities can readily and reliably be obtained, since only the dependence of the parameters on the energy needs be known. Errors entering the measurement were discussed elsewhere.[5,19] The error introduced by calculating differential photoionization cross sections $\sigma_{nl}(\vec{k}, h\nu)$ from the partial cross section $\sigma_{nl}(h\nu)$ in the dipole approximation is small at low photoelectron energies, but may amount to more than 10% for energies between 1 and 3 keV. Hence, the error in the ratio $\sigma_{nl}(\vec{k}, h\nu_1)/\sigma_{nl}(\vec{k}, h\nu_0)$ for lines several 100 eV apart may be of the order of magnitude of 10^{-2}.

F. Linewidth determination

The contour $V(x, \Gamma_V)$ of the observed photoline is the convolution of a Gaussian function $G(x, \Gamma_G)$, representative of the analyzer window function with $\Gamma_G = 0.0015\, E_{\text{kin}}$, and a Lorentzian function $L(x, \Gamma_L)$ characteristic of lifetime-governed natural shapes of levels and x rays. Hence

$$V(x, \Gamma_V) = \int_{-\infty}^{+\infty} L(\xi, \Gamma_L) G(x - \xi, \Gamma_G)\, d\xi, \tag{7}$$

where the Γ's refer to the FWHM of the corresponding contours.

We derived, and used in the data analysis, the analytical expression[20]

$$\frac{\Gamma_L}{\Gamma_V} = 1 - \left(\frac{\Gamma_G}{\Gamma_V}\right)^2 - 0.114\left(1 - \frac{\Gamma_G}{\Gamma_V}\right)\left(\frac{\Gamma_G}{\Gamma_V}\right)^2 \tag{8}$$

for the relation between Γ_L, Γ_G, and Γ_V. Equation (8), which is plotted in Fig. 3, yields values for Γ_L (or Γ_G) that differ by less than 0.1% from those calculated[21] by the exact formula, Eq. (7).

G. Sample preparation and spectrometer operation

The metallic uranium anode was prepared by melting *in vacuo* a disc of uranium metal onto a 0.2-mm tungsten foil, which in turn was silver brazed to the tip of a copper tube. The uranium disc was then reduced to a thickness of 0.3 mm to insure efficient anode cooling. Finally, the sample was filed in argon atmosphere to remove the oxide coating, introduced into the x-ray tube under argon protection, and kept at $p \lesssim 50$ μPa during the measurement. The uranium was of 99% purity as assayed in a wide-scan x-ray fluorescence analysis with a Si(Li) detector.[22] For the calibration runs, silver was evaporated on one half of the target area, so that uranium and silver reference lines could be excited and recorded simultaneously. The uranium oxide anode used to check for possible effects of chemical composition on the x-ray energies was prepared by heating in oxygen[23] a 200-μg/cm^2 uranium sample electrodeposited from isopropyl-alcohol solution on a silver-plated copper anode.

Spectra were excited by 12-keV electrons with a current of either 15–20 mA for the oxide or 40–50 mA for the metal. The anode had a bevel of 10° and the spot size was about 3×5 mm^2. Converter gas pressures were typically 10 Pa in the cell and less than 3 mPa in the analyzer; the Ne 1*s*, Ar 1*s*, and S 1*s* (H_2S) levels were used for conversion. The resolution of the analyzer was set at $\Delta E/E = 0.15\%$ in terms of energy of the electrons entering the dispersive element. The Ag $L\beta_1$ line, $E = 3150.97(3)$ eV, and Ag $L\alpha_1$ line, $E = 2984.34(2)$ eV, served as energy standards.[24]

III. RESULTS AND DISCUSSION

A. Energies of *M* x rays and some *M* and *N* levels

Table I summarizes our results for the stronger lines in the *M* spectrum and also lists the values of Bearden[3] and the data of Lachère.[2] The uncertainties of the present values are considerably

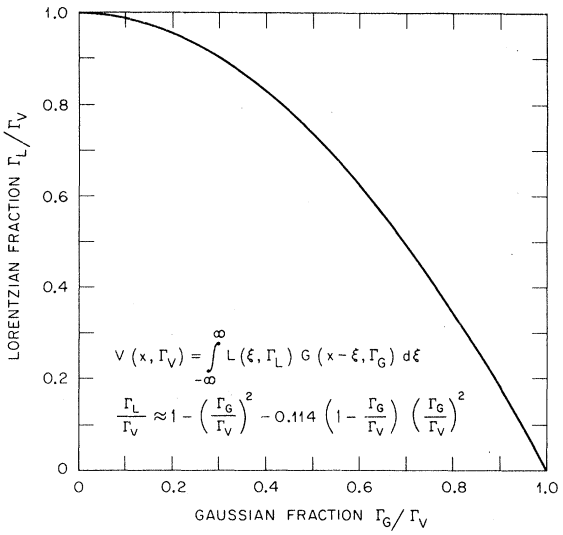

FIG. 3. Lorentzian and Gaussian fractions of the half-width (FWHM) of a Voigt-profile line. Plots of integral (exact) and polynomial (approximate) functions coincide on scale shown.

smaller than those of previous determinations and amount to 0.1–0.5 eV. These errors are largely due to the errors in the determinations of the peak positions. The splitting of the $M\alpha$ doublet is 11.4(5) eV and slightly higher than the value of 10.8(1) eV found for the $4f$ doublet by more accurate photoelectron spectrometric measurements.[25] According to Bonnelle and Lachère,[26] the position of the $M_3N_5\gamma$ line may possibly be affected by interference with other lines. A value of 3171.2(2) eV for $M\alpha_1$ was obtained for the oxide and 3171.4(1) eV for the metal, indicating that the chemical shift lies within the error limits of the measurements.

Using the transition energies of Table I, column 2, and the N_6 and N_7 level energies reported by Fuggle *et al.*[27] for uranium metal, the energies of the M_4, M_5, N_2, and N_3 levels in the metal can be derived. These level energies are entered in Table II with data[17] *presumably* pertaining to oxide and recent data[28] for UO_2. As a measure of the consistency among the sets of data, the differences between the energy values for metal and oxide are also given in Table II. Inferring an energy shift of slightly more than 3 eV to pertain throughout, the N_3 energy of Ref. 27 for the metal appears to be too high by about 1 eV and the M_4 energy of Ref. 29 for the oxide to be more accurate than that of Ref. 17.

B. Linewidths

In Table III experimental and theoretical line widths are tabulated for the strongest lines observed. Also listed are the converter levels whose widths are as follows: Γ(Ne 1s) = 0.23(2) eV[30]; Γ(Ar 1s) = 0.67(2) eV[31]; and Γ(S 1s) = 0.6(1) eV. The width of Γ(S 1s) in H_2S was averaged from the atomic calculations of Refs. 6, 7, and 10 assuming molecular effects to be negligible. A value of 0.6(1) eV was also obtained from analyses of runs in which the $M\beta$ line was converted either by Ar 1s with a well-known level width or by S 1s in H_2S.

The errors quoted include the uncertainties in (a) the widths Γ_γ of the observed lines, (b) widths of converter levels, and (c) the analysis according to Eq. (8) or, alternatively, Fig. 3. In the case of the $M\gamma$ line, no error is given since the degree of line distortion by the M_5 absorption edge is uncertain. Widths of the $M\alpha$ and $M\beta$ lines are found to be slightly less than the theoretical prediction, indicating that theory overestimates the M_4 and M_5 level widths since the N_6 and N_7 levels contribute only about 0.3 eV. On the other hand, the experimental $M\zeta$ line widths are greater than the theoretical widths suggesting that lifetime broadening may not be the sole contributor. Other

TABLE I. Energies of prominent uranium M x rays (in eV).

Line	This work [a]	Bearden [b]	Lachère [c]
$M_5N_3\zeta_1$	2506.8(2)	2506.7(1.0)	2507
$M_5N_6\alpha_2$	3160.0(5)	3159.6(8)	3162
$M_5N_7\alpha_1$	3171.4(1)	3170.9(8)	3172
$M_4N_2\zeta_2$	2455.7(3)	2455.1(1.0)	···
$M_4N_6\beta$	3336.7(1)	3336.4(9)	3336.2
$M_3N_5\gamma$	3565.1(3)	3564(1)	3564.2

[a] Reference lines: Ag $L\beta_1$, 3150.97(3) eV; Ag $L\alpha_1$, 2984.34(2) eV (Ref. 3). Errors indicated in parentheses are standard errors.
[b] Reference 3; probable errors are given.
[c] Reference 2.

TABLE II. Energies of several M and N levels in uranium metal and oxide (in eV).

Level	Metal	Oxide [a]	UO_2	Δ Oxide–Metal
M_4	3724.9(3) [b]	3727.6(3)	···	2.7; (3.2) [f]
M_5	3548.8(3) [b]	3551.7(3)	···	2.9
N_2	1269.2(5) [b]	1272.6(3)	···	3.4
N_3	1042.0(4) [b] 1043.0(6) [c]	1044.9(3)	···	2.9 1.9
N_4	···	780.4(3)	780.1(5) [d]	···
N_5	···	737.7(3)	737.7(5) [d]	···
N_6	388.2(1) [c]	391.3(6)	390.8(4) [e]	3.1; 3.5
N_7	377.4(1) [c]	380.9(9)	380.0(4) [e]	3.5; 3.6

[a] Bearden and Burr (Ref. 17); best-fit values; undefined oxides.
[b] This work in reference to N_6 and N_7 energies.
[c] Fuggle *et al.* (Ref. 27).
[d] Veal *et al.* (Ref. 28).
[e] Weighted average (Ref. 28).
[f] Using $E(M_4)$ = 3728.1 eV reported by Nordling and Hagström (Ref. 29).

TABLE III. Widths (FWHM) of uranium M x-ray lines (in eV).

Line	Experiment	Theory [a]	Converter level
$M_5N_3\zeta_1$	15(2)	10.81	Ne 1s
$M_5N_6\alpha_2$	4.1(6)	4.47	S 1s of H_2S; (Ne 1s)
$M_5N_7\alpha_1$	4.1(3)	4.47	S 1s of H_2S; (Ne 1s)
$M_4N_2\zeta_2$	13(2)	11.91	Ne 1s
$M_4N_6\beta$	4.3(3)	4.74	Ar 1s
$M_3N_5\gamma$	14 [b]	16.77	Ne 1s

[a] M levels from Ref. 8; N levels from Ref. 9. Nonrelativistic Hartree-Slater calculations.

[b] Line distorted by M_5 absorption edge (see Fig. 5).

effects,[5,18] such as satellite overlap and multiplet splitting, may be the cause of the additional broadening.

In Fig. 4 an interesting case is displayed, in which the line width Γ_L of $M\beta$ is given simply by $\Gamma_L = \Gamma_V - \Gamma_L(\text{Ar } 1s)$, since the window width, $\Gamma_G = 0.0015\, E_{\text{kin}}$, is negligibly small.

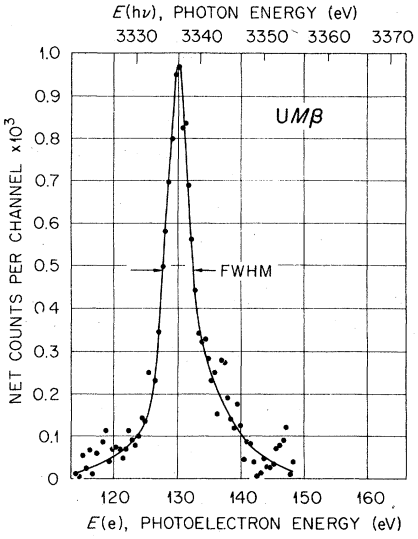

FIG. 4. $M\beta$ line of uranium converted by the Ar 1s level into a photoline of low energy having negligible instrumental (Gaussian) broadening.

C. Relative intensities

The relative intensities were deduced from the photoelectron spectrum obtained with Ne 1s as a converter and with no preacceleration (Sec. II E) using the procedures outlined in Ref. 5. From the observed spectrum, Fig. 5, a constant background consisting of bremsstrahlung, detector noise, and stray electrons, and the contributions from inelastic scattering and shakeup were subtracted, and the resulting *line* spectrum was transformed into the x-ray line spectrum with the aid of Eq. (6). The energy dependence of the detector efficiency η was taken from Bordoni,[32] α was assumed to be constant, and the energy dependences of Γ and $\sigma_{nl}(\vec{k}, h\nu)$ were calculated from known total cross sections σ_{tot}.[33,34] For the neon converter, we used[34] $\sigma_{1s}(h\nu) = 0.729\, \sigma_{\text{tot}}(h\nu)$ and $\sigma_{1s}(\vec{k}, h\nu) \propto \sigma_{1s}(h\nu)$ incurring a small error by the neglect of retardation. The relative x-ray intensities, observable at a mean takeoff angle of 10° are listed in Table IV. These intensities need to be corrected for self-absorption in the target to arrive at relative emission rates and branching ratios that can be compared with theory. Approximate correction factors, which are also listed in Table IV, were calculated using Feldman's expression[35] for the electron range and Scofield's relativistic cross sections.[36] The experimental branching ratios are found to be in poor accord with the nonrelativistic calculation[37]

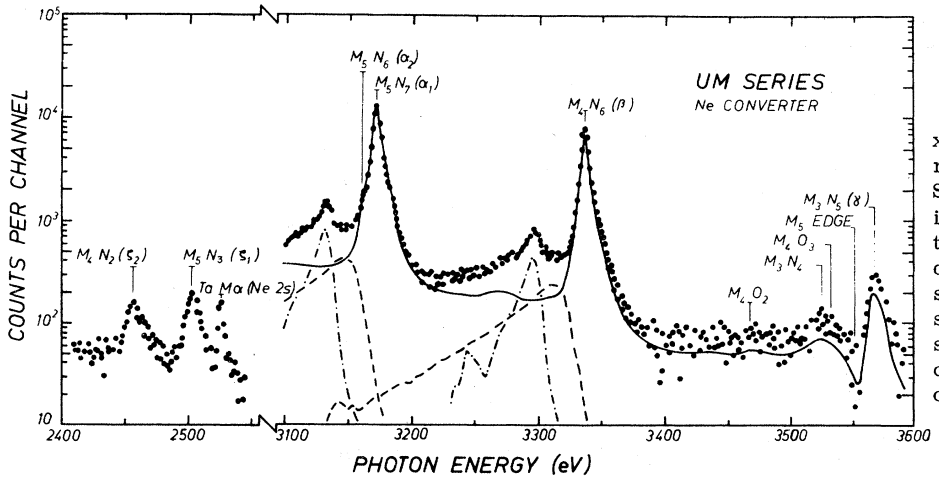

FIG. 5. Uranium M x-ray spectrum showing the major emission lines. Spectrum corrected according to Eq. (6) after subtraction of shakeup (dash-dot lines) and inelastic scattering (dash lines) structures is shown as a solid line. Tantalum line comes from filament shield of x-ray tube.

TABLE IV. Relative intensities of U M x rays excited by 12-keV electrons, and branching ratios for M_4 and M_5 shells.

Line	Rel. intensity Expt.	Correction factor [a]	Branching ratios Expt. [b]	Theory Rel. [c]	Theory nonrel. [d]
$M_5N_7\alpha_1$	100	1.00	100	100	100
$M_5N_6\alpha_2$	2.6(3)	1.01	2.6(3)	5.1	5.0
$M_5N_3\xi_1$	3.3(7)	1.66	5.5(1.3)	3.3	2.3
$M_4N_6\beta$	49(2)	0.92	100	100	100
$M_4N_2\xi_2$	3.1(7)	1.74	11(3)	4.6	1.7
M_4O_2	0.4(2)	0.83	0.8(5)	1.0	0.4
$M_3N_5\gamma$	2.4(4)	1.83 [e]	...	...	...

[a] For target self-absorption; see e.g., Ref. 5.
[b] Error includes estimated uncertainties in correction factors.
[c] Reference 38, interpolated values.
[d] Reference 37.
[e] Not considering finer details near the M_5 edge.

and only in fair agreement with the relativistic Hartree-Slater calculation of Bhalla.[38]

D. Satellites

The high-energy satellites that accompany the $M\alpha_1$ and $M\beta$ lines were isolated by fitting Voigt profiles [Eq. (7)] to the parent lines. As shown in Fig. 6, broad satellite bands were obtained whose intensities are 11(2)% relative to the respective $M\alpha_1$ and $M\beta$ lines. In analogy to the results of an analysis of the Zr L spectrum,[5] these satellite lines clustering 6–12 eV above the parent lines are due to x-ray transitions in double-hole configurations created predominantly by Coster-Kronig transitions in the M shell. Radiative transitions in the presence of the preferably created $M_{4,5}N$ hole states were calculated[39] to have energies 6–10 eV greater than the diagram lines. By contrast, shakeoff, another process producing double-hole satellites, creates an additional hole mostly in the O, P, and Q shells with the consequence that the resulting satellites will coincide with the diagram lines. As detailed in Tables V and VI, which summarize the relevant shakeoff probabilities[39] and energy shifts, over 20% of the $M\alpha$ and $M\beta$ line intensities are due to shakeoff satellite contributions. An additional percentage comes from Coster-Kronig generated $M_{4,5}N$ holes in which the N vacancy is transferred to O or P shells before the radiative decay of the $M_{4,5}$ vacancy.[5,40] The large number of satellite lines mixed in with the diagram lines may also influence the symmetry, the width, and the energy

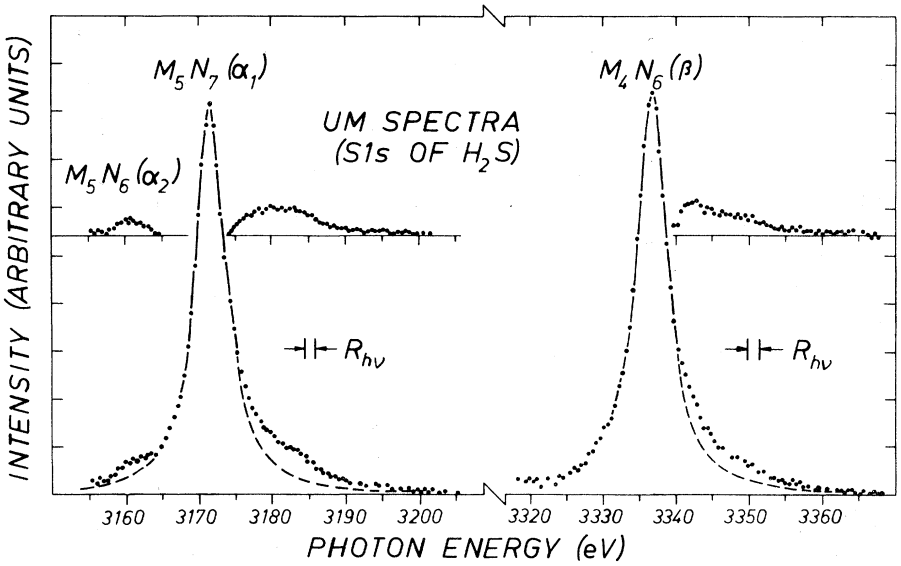

FIG. 6. $M\alpha_1$ and $M\beta$ lines of uranium fitted with a Voigt function resulting in the separation of the high-energy satellite bands and the $M\alpha_2$ line shown in the insets. Spectrometer resolution, which includes window and converter-level widths, is denoted by $R_{h\nu}$. 12-keV electron excitation.

TABLE V. Energy shifts (eV) of double-hole satellites relative to their parent $M\alpha_1$ and $M\beta$ Lines of uranium calculated from relativistic Hartree-Slater total-energy differences (Ref. 39).

Level of the second hole X_i	α_1 satellites $M_5X_i \rightarrow N_7X_i$	β satellites $M_4X_i \rightarrow N_6X_i$
M_3	44.4	45.5
M_4	55.4	57.1
M_5	53.0	54.6
N_1	9.4	9.5
N_2	10.0	10.2
N_3	7.5	7.5
N_4	8.4	8.6
N_5	7.7	7.9
N_6	7.4	7.2
N_7	6.9	6.6
O_1	0.9	0.9
P_1	0.0	0.1
Q_1	−0.1	0.0

position of a line and hence may determine, even in the absence of multiplet splitting, the ultimate accuracy that can be achieved in a measurement of the various single-particle properties.

IV. SUMMARY

Energies, natural widths, and relative intensities of the major M x-ray lines of uranium were measured and the energies of the M_4, M_5, N_2, and N_3 levels in metallic uranium were obtained. X-ray energies were determined with higher accuracy in this work than were reported before. Hartree-Slater predictions of the widths agree satisfactorily with the experimental results.

TABLE VI. Total and partial shakeoff probabilities for the sudden removal of an electron from the different M subshells of uranium calculated with RHS wave functions (Ref. 39).

Initial vacancy	Shells M	N	O	P	Q	Total
M_1	0.011	1.09	6.28	7.55	8.48	23.4
M_2	0.014	1.13	6.32	7.59	8.49	23.5
M_3	0.008	1.03	6.23	7.53	8.47	23.3
M_4	0.016	1.21	6.35	7.60	8.48	23.7
M_5	0.014	1.13	6.32	7.57	8.48	22.4

Branching ratios calculated relativistically show only fair agreement with the experimental ratios. Origin and effects of the satellites, especially those contributing to the diagram lines were briefly discussed, and calculated shakeoff probabilities for M shell ionization are reported along with the calculated relative energies of the various satellites.

In this work the PAX method has proven to be of merit at higher x-ray energies than previously measured. All pertinent parameters of the stronger x-ray lines could readily be determined.

ACKNOWLEDGMENTS

The authors are indebted to Dr. C. W. Nestor, Jr. for calculating shakeoff probabilities and x-ray satellite energies. One of us (O.K-R.) gratefully acknowledges the support by the Jenny ja Antti Wilhurin rahasto and Emil Aaltosen Säätiö grants, and by AEC Contract No. AT-(40-1)-4447 with the University of Tennessee.

*Research sponsored by the U. S. Energy Research and Development Administration under contract with Union Carbide Corporation.

†Permanent address: Laboratory of Physics, Helsinki University of Technology, 02150 Otaniemi, Finland.

[1]W. Stenström, Dissertation (Lund, 1919) (unpublished); E. Hjalmar, Z. Phys. 15, 65 (1923); E. Lindberg, Nova Acta R. Soc. Sci. Ups. 7, No. 7 (1931); W. C. Pierce and A. V. Grosse, Phys. Rev. 47, 532 (1935).

[2]G. Lachère, C. R. Acad. Sci. B 267, 821 (1968).

[3]J. A. Bearden, Rev. Mod. Phys. 39, 78 (1967).

[4]M. O. Krause, Adv. X-Ray Anal. 16, 74 (1973); Physica Fennica, 9, S1-281 (1974); M. O. Krause and J. G. Ferreira, J. Phys. B 8, 2007 (1975).

[5](a) M. O. Krause, F. Wuilleumier, and C. W. Nestor, Jr., Phys. Rev. A 6, 871 (1972); (b) M. O. Krause and F. Wuilleumier, in *Proceedings of the International Conference on Inner Shell Ionization Phenomena and Future Applications, Atlanta, Georgia, 1972,* edited by R. W. Fink, S. T. Manson, J. M. Palms, P. V. Rao, CONF-720404 (Natl. Tech. Information Service, U.S. Dept. of Commerce, Springfield, Va., 1973), p. 2331.

[6]J. H. Scofield, Phys. Rev. A 9, 1041 (1974).

[7]E. J. McGuire, Phys. Rev. A 2, 273 (1970).

[8]E. J. McGuire, in Ref. 5(b), p. 662.

[9]E. J. McGuire, Phys. Rev. A 9, 1840 (1974).

[10]V. O. Kostroun, M. H. Chen, B. Crasemann, Phys. Rev. A 3, 533 (1971).

[11]O. Keski-Rahkonen and M. O. Krause, Physica Fennica 9, S1-261 (1974).

[12]Because of $(V_1 + V_0)$ the correction is important even for small $\Delta V = V_1 - V_0$.

[13]Assuming infinitely long slits. A. J. H. Boerboom, Z. Naturforsch. 14A, 809 (1959); 15A, 244 (1960); and 15A, 253 (1960).

[14]E. M. Purcell, Phys. Rev. 54, 818 (1938).

[15]K. D. Sevier, *Low Energy Electron Spectrometry* (Wiley-Interscience, New York, 1972), p. 20.

[16]T. D. Thomas, R. W. Shaw, Jr., J. Electron. Spectrocs. 7, 1081 (1974) for neon data.

[17]J. A. Bearden and A. F. Burr, Rev. Mod. Phys. 39,

125 (1967).
[18]M. O. Krause, in *Atomic Innershell Processes*, edited by B. Crasemann (Academic, New York, 1975), Vol. II, p. 33.
[19]F. Wuilleumier and M. O. Krause, Phys. Rev. A 10, 242 (1974).
[20]A similar expression was derived by J. F. Kielkopf, J. Am. Opt. Soc. 63, 987 (1973).
[21]See, for example, J. T. Davies, J. M. Vaughan, J. Astrophys. 137, 1302 (1963).
[22]We are indebted to L. D. Hulett of ORNL for this analysis.
[23]The treatment chosen favored the U_3O_8 oxide.
[24]Taken from wavelengths tables of Ref. 3 using the Å*-to-Å conversion factor by R. D. Deslattes and A. Henins [Phys. Rev. Lett. 31, 1972 (1973)], and *hc* value by B. N. Taylor, W. H. Parker, and D. N. Langenberg [Rev. Mod. Phys. 41, 375 (1969)].
[25]We find a value of 10.7(2) eV by operating the instrument in the PAL mode (Ref. 18); B. W. Veal *et al*. (Ref. 28) report 10.9 eV, and others [see J. Verbist *et al*. (Ref. 28)] find 10.8 eV.
[26]C. Bonnelle and G. Lachère, J. Phys. (Paris) 35, 295 (1974); C. Bonnelle, Physica Fennica 9, S1-92 (1974).
[27]J. C. Fuggle, A. F. Burr, L. M. Watson, D. J. Fabian, W. Lang, J. Phys. F 4, 335 (1974).
[28]B. W. Veal, D. J. Lam, H. Diamond, and H. R. Hoekstra, Phys. Rev. B (to be published); J. Verbist, J. Riga, J. J. Pireaux, R. Caudano, J. Electron. Spectrosc. 5, 193 (1974); G. C. Allen and P. M. Tucker, J. Chem. Soc. Dalton Trans. 5, 470 (1973).
[29]C. Nordling and S. Hagström, Ark. Fys. 15, 431 (1959).
[30]U. Gelius, S. Svensson, H. Siegbahn, E. Basiliv, Å. Faxälv, and K. Siegbahn, Chem. Phys. Lett. 28, 1 (1974).
[31]T. Watanabe, Phys. Rev. 139, A1747 (1965).
[32]F. Bordoni, Nucl. Instrum. Meth. 97, 405 (1971).
[33]B. L. Henke and R. L. Elgin, Adv. X-Ray Anal. 13, 639 (1970).
[34]F. Wuilleumier, Adv. X-Ray Anal. 16, 63 (1973).
[35]C. Feldman, Phys. Rev. 117, 455 (1960).
[36]J. H. Scofield, UCRL-51326 report (1973), p. 313.
[37]S. T. Manson and D. J. Kennedy, At. Nucl. Data Table 14, 111 (1974). Values apportioned according to E. V. Condon and G. H. Shortley, *The Theory of Atomic Spectra* (Cambridge U.P., London, 1959), p. 243.
[38]C. P. Bhalla, J. Phys. B 3, 916 (1970).
[39]Courtesy of C. W. Nestor, Jr.
[40]F. Wuilleumier and M. O. Krause, in *Proceedings of the International Conference on X-Ray Spectra and Electronic Structure of Matter*, edited by A. Fässler and G. Wiech (Universität München, 1973), p. 397.